molecular pharmaceutics

ACS AuthorChoice

Article

pubs.acs.org/molecularpharmaceutics

Terms of Use

Adjuvant Cationic Liposomes Presenting MPL and IL-12 Induce Cell Death, Suppress Tumor Growth, and Alter the Cellular Phenotype of Tumors in a Murine Model of Breast Cancer

Ismail M. Meraz,[†] David J. Savage,[†,‡,∥] Victor Segura-Ibarra,[†,§] Jeffrey Li,[†] Jessica Rhudy,[†] Jianhua Gu,[†] and Rita E. Serda*[,†,§,∥]

[†]Department of Nanomedicine, Houston Methodist Research Institute, Houston, Texas 77030, United States

[‡]University of Texas School of Medicine, Houston, Texas 77030, United States

[§]Escuela de Biotecnología y Alimentos, Escuela de Medicina y Ciencias de la Salud Instituto Tecnológico de Estudios Superiores de Monterrey, Monterrey, NL 64710, Mexico

[∥]Michael E. DeBakey Department of Surgery, Baylor College of Medicine, Houston, Texas 77030, United States

ABSTRACT: Dendritic cells (DC) process and present antigens to T lymphocytes, inducing potent immune responses when encountered in association with activating signals, such as pathogen-associated molecular patterns. Using the 4T1 murine model of breast cancer, cationic liposomes containing monophosphoryl lipid A (MPL) and interleukin (IL)-12 were administered by intratumoral injection. Combination multivalent presentation of the Toll-like receptor-4 ligand MPL and cytotoxic 1,2-dioleoyl-3-trmethylammonium-propane lipids induced cell death, decreased cellular proliferation, and increased serum levels of IL-1β and tumor necrosis factor (TNF)-α. The addition of recombinant IL-12 further suppressed tumor growth and increased expression of IL-1β, TNF-α, and interferon-γ. IL-12 also increased the percentage of cytolytic T cells, DC, and F4/80$^+$ macrophages in the tumor. While single agent therapy elevated levels of nitric oxide synthase 3-fold above basal levels in the tumor, combination therapy with MPL cationic liposomes and IL-12 stimulated a 7-fold increase, supporting the observed cell cycle arrest (loss of K_i-67 expression) and apoptosis (TUNEL positive). In mice bearing dual tumors, the growth of distal, untreated tumors mirrored that of liposome-treated tumors, supporting the presence of a systemic immune response.

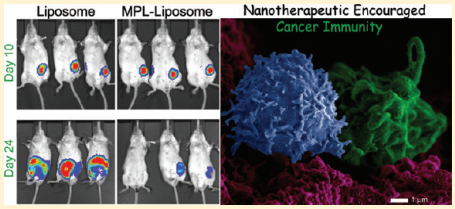

KEYWORDS: *liposome, monophosphoryl lipid A, interleukin-12, Toll-like receptor, breast cancer*

INTRODUCTION

The goal of cancer immunotherapy is to boost or restore immune function for effective recognition of antigens associated with aberrant cells. The range of immunotherapy approaches is broad and includes antibody therapy,[1] cytokine delivery to stimulate a passive immune response,[2,3] *ex vivo* stimulation of autologous immune cells that are subsequently administered to a patient,[4] the use of toxic chemotherapy agents for stimulating an immune response,[5] and formulations consisting of antigens combined with alum, emulsions, liposomes, immune stimulating complexes,[6] or polymeric nanoparticles.[7]

Beyond protective transport and sustained release of therapeutics, nanoparticles and particulates have intrinsic properties that impact biological outcomes. As an example, the vaccine adjuvant alum, thought to function as a depot for sustained antigen release, induces cytotoxic effects leading to the release of uric acid and recruitment of immune cells to the site of injection.[8] Alum favors T helper 2 (Th2) immune responses, which induce B cells to produce neutralizing antibodies.[9−11] However, effective cancer immunotherapies require Th1 cytokines to arrest tumor growth, specifically IFN-γ and TNF-α.[12]

Similar to alum, cationic liposomes have inherent cytotoxicity, inducing cell death and stimulating immune cell infiltration to the site of injection or accumulation. However, in contrast to alum, which relies on surface absorption for binding of substrates, such as MPL, liposomes incorporate MPL into the lipid bilayer. Previously, we reported that MPL liposomes suppress tumor growth in a 4T1 immune competent murine model of breast cancer, unlike an equivalent dose of free MPL.[13] In addition to recruiting and activating immune cells, tumor cell damage caused by the cationic liposomes is proposed to release endogenous tumor antigens, directing the immune response against cancer cells. The large pool of endogenous tumor antigens creates an array of epitopes for immune recognition.The adjuvant effects of cationic liposomes are supported by Yan et al.[14] who demonstrated by microarray mRNA analysis that DOTAP liposomes up-regulate chemokines, including CCL2, CCL3, and CCL4 in dendritic cells (DC). Barnier-Quer et al.[15] demonstrated that incorporation of cholesterol in the bilayer of cationic liposomes enhances their adjuvant effect. We previously demonstrated using porous silicon microparticles that particle presentation of adsorbed MPL (i.e. multivalent presentation) increases particle uptake by

Received: April 13, 2014
Revised: August 24, 2014
Accepted: September 1, 2014
Published: September 1, 2014

DC; elevates DC expression of costimulatory and major histocompatibility complex (MHC) class I and II molecules; increases migration of DC to the draining lymph node; and enhances associations between DCs presenting the ovalbumin peptide SIINFEKL and T cells from OT-1 mice.[16]

The goal of this project is to elicit cancer-specific *de novo* host immune responses through injection of tumors with cationic adjuvant liposomes. We examine the *in vivo* immunomodulatory properties of liposomes containing MPL and recombinant IL-12 (rIL-12) using an immune competent 4T1 mouse model of breast cancer. The impact of adjuvant liposomes on cell viability and tumor growth are explored, as is the impact of the particles on the cytokine milieu and immune cell phenotype of the tumor.

EXPERIMENTAL SECTION

Materials. MPL from *Salmonella enteric* serotype Minnesota RE 595 and cholesterol (Sigma grade ≥99%) were purchased from Sigma-Aldrich (St. Louis, MO, USA). 1,2-Dipalmitoyl-*sn*-glycero-3-phosphocholine (DPPC) and 1,2-dioleoyl-3-trimethylammonium-propane (DOTAP) chloride salt were obtained from Avanti Polar Lipids, Inc. (Alabaster, AL, USA). Mouse Novex Cytokine Magnetic 10-Plex ELISA kits were purchased from Invitrogen (Grand Rapids, NY, USA). 4T1-luc2-td Tomato Bioware Ultra Red mouse mammary cancer cells were purchased from Caliper Life Sciences (Hopkinton, MA, USA). Recombinant mouse IL-12 was purchased from R&D Systems, Inc. (Minneapolis, MN, USA).

Animals. BALB/c mice (6−8 wk old) were obtained from Charles River Laboratories, Inc. (Wilmington, MA, USA). All procedures were performed in accordance with protocols reviewed and approved by the Institutional Animal Care and Use Committee at Houston Methodist Research Institute.

Preparation and Characterization of Liposomes. DOTAP liposomes were prepared using a molar ratio of 7:3:1 for DPPC/cholesterol/DOTAP. Lipids (40 mg) were dissolved in a 3 mL chloroform/methanol (3:1) solution, and 250 μg of MPL, dissolved in chloroform at 5 mg/mL, was added. Organic solvent was removed by overnight heating at 55 °C in a Hei-Vap Series Heidolph Rotatory Evaporator (Schwabach, Germany). The liposomes were recovered in 2 mL of PBS, followed by heating in a water bath at 52 °C for 3 min, then vortexing for 3 min and sonication for 30 s. The heat, vortex, and sonication cycle was repeated 3 times followed either by final sonication for 3 min to get the final liposome product or by extrusion through dual filters (200 nm), 8×, using a 10 mL Thermobarrel Extruder from Northern Lipids, Inc. (Burnaby, B.C., Canada). For liposomes containing cytokine, IL-12 was added to the hydrating PBS at a final concentration of 0.1 mg/mL. Adsorption of IL-12 to the liposomes was determined by quantitating the amount of IL-12 depleted from the solvent after removal of the liposomes by centrifugation using the BD Cytometric Bead Assay for mouse IL-12p70 (San Diego, CA, USA). Size and charge of liposomes were characterized by dynamic light scattering (DLS) and zeta potential analysis using a Malvern Zetasizer (Worcestershire, U.K.). Liposome size and shape were further characterized by atomic force microscopy (AFM) using a Bruker Multimode SPM system (Santa Barbara, CA, USA). AFM images were acquired in PBS in contact mode using MLCT cantilevers purchased from Bruker with a spring constant at 0.01 N/m.

Cytotoxicity Studies. The cytotoxicity of cationic liposomes to 4T1 breast cancer cells was evaluated by flow cytometry using propodium iodide (PI). Using a 24-well plate format, cells were treated with 4 μg of control or MPL liposomes, or free MPL (250 ng) for 24 h. Cells were released using trypsin and treated with PI according to the manufacturer's protocol (Invitrogen). Samples were analyzed using a LSR II Flow Cytometer (BD Biosciences, Mountain View, CA, USA) equipped with FACSDIVA software.[17] *In vivo* tumor cytotoxicity of cationic liposomes was evaluated in BALB/c mice bearing 200 mm^3 4T1 tumors 24 h following intratumoral injection of liposomes (50 μL; 1 mg of lipid). Excised tumors were embedded in paraffin, sectioned, and stained with hematoxylin and eosin (H&E) or used for analysis of apoptosis using the DeadEnd Fluorometric TUNEL System (Promega, Madison, WI, USA).

Multiplex Bead ELISA. Serum cytokines were analyzed 5 h after intratumoral injection of liposomes using a mouse cytokine magnetic 10-plex panel kit (Invitrogen, Carlsbad, CA, USA) for the Luminex platform. Following retro-orbital eye bleed, plasma was collected by centrifugation at 1500*g* for 10 min at 4 °C and stored at −80 °C. Plates were prepared using 25 μL/well of the antibody-bound bead. After 2 washes, 50 μL serum and 50 μL assay diluent (or 100 μL standard) were added and plates were incubated at room temperature for 2 h on an orbital shaker. After two washes, 100 μL of biotinylated detector antibody was added to the beads, and they were incubated for an additional hour, followed by two more washes and the addition of 100 μL of streptavidin-RPE for 30 min. After a final two washes, beads were suspended in 125 μL of wash solution and inserted into the XY platform of a Luminex MAGPIX Instrument (EMD Millipore, Billerica, MA, USA). The assay protocol was designed using xPONENT software and samples were run at 100 events/bead region.

Immunhistochemistry. Tissues were quick frozen in OCT (Tissue-Tek) and stored at −80 °C. Tissue sections (10 μm) were fixed with ice-cold acetone for 15 min at −20 °C and washed three times with 1× PBS followed by blocking with 5% fetal bovine serum in PBS. Fluorescence-labeled antibodies [e-flour 615 CD8 (clone 53-6.7; 1:50), e-flour 570 K_i-67 (clone solA15; 1:100; eBioscience, San Diego, CA, USA); FITC F4/80 (MCA497A488;1:100); Alexa Fluor 647 CD204 (MCA1322; 1:100, AbD Serotec, Raleigh NC, USA); 33D1 (1:100, BD Biosciences, San Jose, CA; 1:500 secondary antirat IgG Alexa Fluor 546; Invitrogen); and iNOS (6/iNOS/NOS; 1:100 BD Biosciences, San Jose, CA, USA; 1:500 antirabbit IgG-TRITC, Jackson Immunoresearch Laboratories, Inc. West Grove, PA, USA)] were incubated with tissues overnight at 4 °C in the presence of 5% FBS. Slides were then washed three times with PBS and mounted with ProLong Gold AntiFade with DAPI (Invitrogen). Images were taken using an A1 Nikon confocal microscope, and the percent positive cells were determined by manual counting of four arbitrary regions in random samples.

Therapeutic Efficacy Studies. Breast cancer tumors were established in BALB/c mice by intramammary injection of 1×10^5 4T1-luciferase cells. When tumors reached a median size of 100−200 mm^3, mice were administered intratumoral injections as follows: PBS control, free MPL (6.25 μg), control liposomes (50 μL; 1 mg of lipid); MPL liposomes (50 μL), and IL-12 (5 μg) with/without MPL liposomes. Tumor growth was monitored by caliper measurements three times per week and by luciferase expression measured weekly using the Xenogen IVIS-200 System (PerkinElmer Inc., Waltham, MA, USA) following intraperitoneal injection of 75 mg/kg RediJect D-Luciferin (PerkinElmer Inc.). Then, 24−26 days after initiation of tumor growth, mice were sacrificed, blood was collected by retro-orbital bleeding, and tumor and spleen were collected for

dx.doi.org/10.1021/mp5002697 | *Mol. Pharmaceutics* 2014, 11, 3484−3491

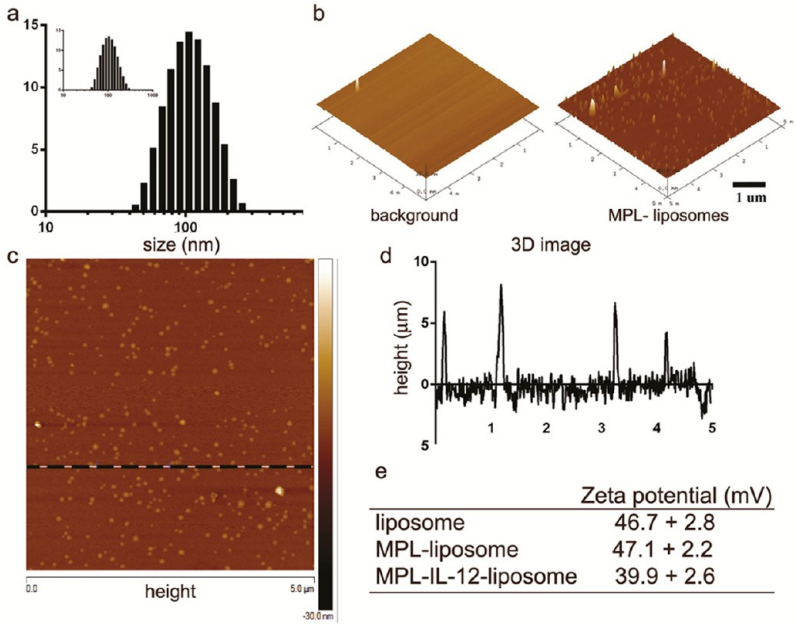

Figure 1. Characterization of liposomes. (a) Dynamic light scattering was used to assess particle size. The size distribution of MPL liposomes is shown, with the inset showing the size distribution of control liposomes. (b) Three-dimensional atomic force microscopy images show the surface topography of an oxidized silicon chip before and after binding of MPL liposomes. (c) Two-dimensional height images showing a homogeneous population of MPL liposomes. The height of particles lying on the line is displayed in the spectra in panel d. (e) Zeta potential of each liposome population.

immunohistochemical, weight, and size analysis. Dual tumors were grown in naïve mice using the same experimental conditions with intratumoral injection of particles limited to a single tumor.

RESULTS

Characterization of Cationic MPL Liposomes. In order to create localized necrosis for release of tumor antigens and uric acid, we created a cationic liposome embedded with the TLR-4 ligand MPL. MPL favors the release of cytokine signatures supporting tumor regression. Dynamic light scattering (Figure 1a) supported an average diameter of 100.3 ± 0.43 and 103.3 ± 1.85 nm for control and MPL-loaded liposomes, with a poly dispersity index of 0.115 ± 0.014 and 0.28 ± 0.01, respectively. To evaluate the heterogeneity of the population, liposomes were bound to an oxidized silicon wafer, with 3D images of the wafers displayed in Figure 1b. The height image of the MPL liposomes (Figure 1c) supported a disperse population that was uniform in size. A line scan through the height image also supported homogeneity in size (Figure 1d). The surface potential of the liposomes was approximately 47 mV for both control and MPL liposomes (Figure 1e). The addition of rIL-12 to the liposomes reduced the surface potential by 7 mV, supporting surface adhesion by rIL-12. Based on detection of unbound IL-12 using a Mouse IL-12p70 Enhanced Sensitivity Flex Set from BD Biosciences (R^2 = 0.987 for standard curve), 34% and 26% of cytokine was in the bound state when introduced to control or MPL containing liposomes, respectively.

Evaluation of Liposome Cytotoxicity. To study particle cytotoxicity, 4T1 cells were cultured with 4 μg/mL liposomes for 24 h, and cell death was measured by flow cytometry based on propodium iodide (PI) uptake. Control and MPL liposomes induced cell death in 93% and 95% of the cells, whereas control and free MPL treated cells displayed 14% and 16% cell death, respectively (n = 3; Figure 2a). Flow cytometry histograms of the FL2 orange−red channel show a shift in the entire population of liposome-treated cells (Figure 2b).

The *in vivo* cytotoxicity of the cationic liposomes was studied in BALB/c 4T1 orthotopic tumors. When the tumor volumes reached 100−200 mm^3, intratumoral injections with PBS, free MPL, or liposomes were performed. After 24 h, the mice were sacrificed, and tumor tissue was analyzed by H&E and TUNEL staining. In contrast to untreated tumors, clear necrotic regions were visible in mice treated with MPL liposomes (Figure 2c). While minimal cell death was present in untreated tumors and tumors treated with MPL based on TUNEL staining abundant cell death was present after treatment with both control and MPL liposomes (Figure 2d).

Therapeutic Efficacy of Cationic Adjuvant Liposomes. To examine the impact of cationic MPL liposomes on breast tumor growth, 4T1 orthotopic breast tumors were established to a size of 100−200 mm^3. Intratumoral injections of liposomes were performed once a week for 2 weeks. Tumor growth was monitored by caliper measurements and luciferase expression using the IVIS Imaging System 200, and tumor weights were measured at the end of study. Despite inducing localized cell death, control cationic liposomes did not reduce the rate of tumor growth (Figure 3a). However, the addition of MPL to the liposomes led to a dramatic reduction in tumor growth. Similar to control liposomes, free MPL did not slow tumor growth (Figure 3b). Bioluminescence imaging of luciferase expression following luciferin injection using the IVIS 200 imaging system supported the caliper data, with MPL liposome treatment blocking tumor progression (Figure 3c). The mass of excised tumors on day 25 support a significant reduction in tumor growth following treatment of MPL liposomes compared to both PBS and control liposome treated mice (Figure 3d).

Combination Adjuvant Therapy Increases Blockade of Tumor Growth. To create a microenvironment conducive

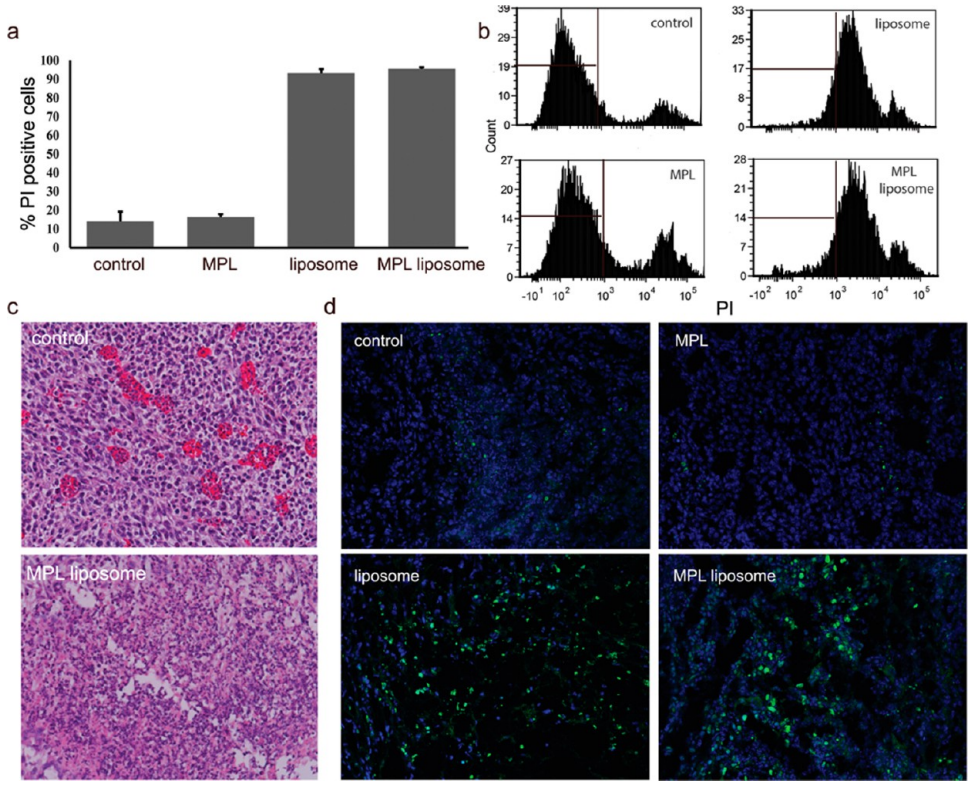

Figure 2. Cytotoxic nature of cationic liposomes. (a) Cell death as measured by propidium iodide uptake in 4T1 cells following a 24 h incubation with 4 μg/mL DOTAP liposomes or 250 ng/mL MPL. (b) Flow cytometry histograms illustrate the impact of MPL and/or liposomes on cell viability. (c) H&E staining of BALB/c 4T1 tumor sections following no treatment (control) or treatment with MPL liposomes. (d) TUNEL staining of tumor sections following treatment of mice bearing 4T1 tumors with MPL or liposomes.

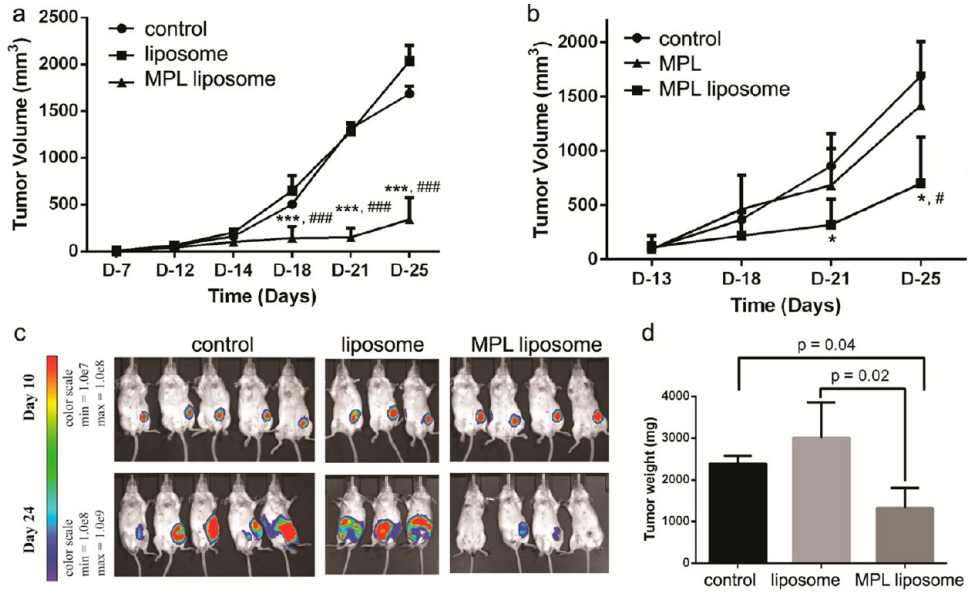

Figure 3. Impact of MPL liposomes on tumor growth. (a) BALB/c mice bearing orthotopic 4T1 tumors were treated with two weekly intratumoral injections of control or MPL liposomes beginning on day 12 after injection of tumor cells (n = 5/group; tumor approximately 200 mm^3). Caliper-derived tumor measurements were taken every 2−4 days (***p = 0.0001 compared to vehicle control; $^{###}p < 0.0001$ compared to liposome control). (b) BALB/c mice bearing 4T1 tumors were also treated with two weekly intratumoral injections of free or liposome-encapsulated MPL beginning on day 13 after intramammary injection of tumor cells (n = 3−5/group), with caliper-derived tumor measurements presented (*$p < 0.05$ compared to vehicle control; $^{#}p < 0.05$ compared to MPL; reprinted with permission from ref 13; copyright 2014 Public Library of Science]. (c) IVIS imaging of tumor cell luciferase expression in mice following intraperitoneal injection with luciferin (75 mg/kg) before and after liposome treatment. (d) Mean weight of excised tumors on day 25.

dx.doi.org/10.1021/mp5002697 | Mol. Pharmaceutics 2014, 11, 3484−3491

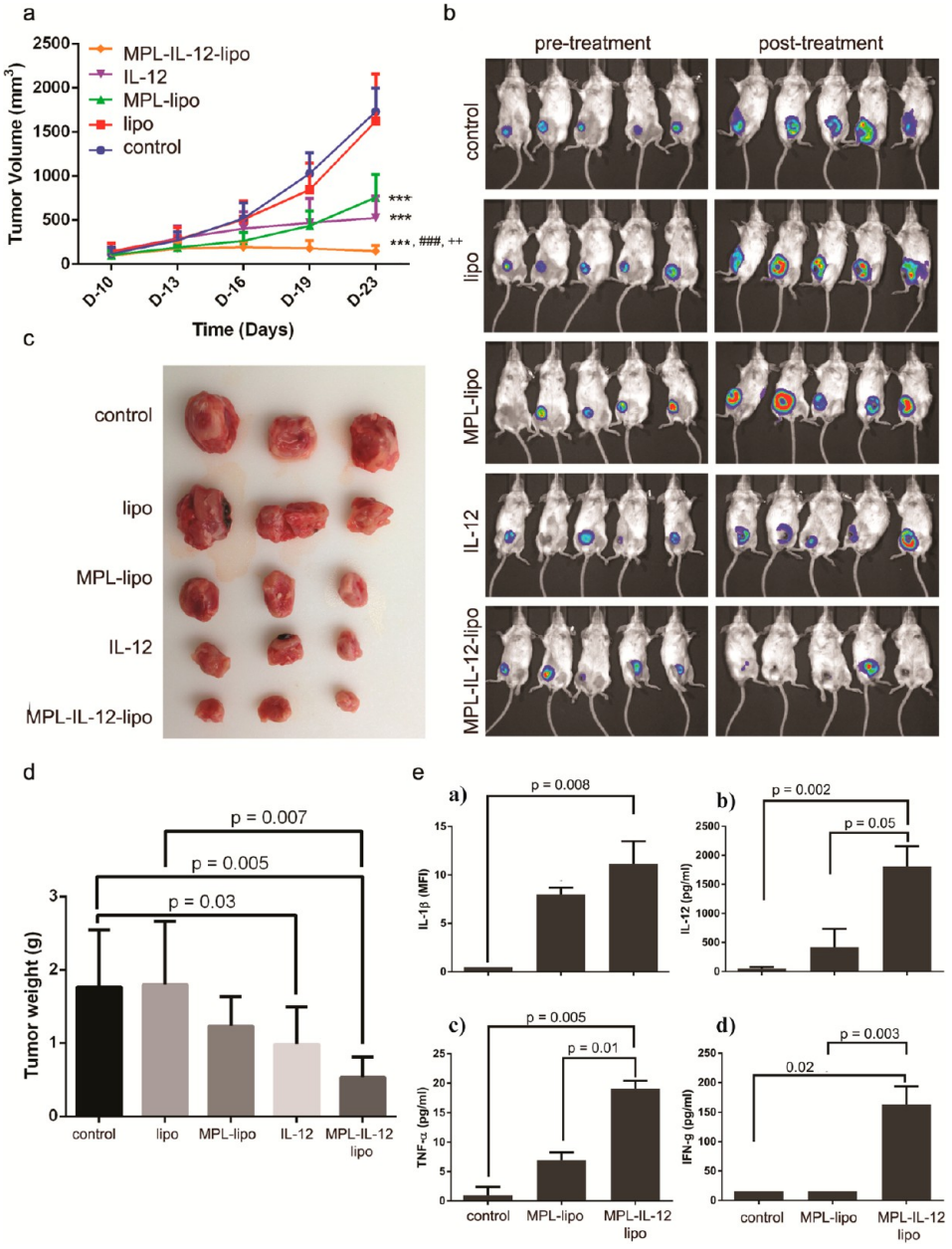

Figure 4. Influence of IL-12 on the therapeutic efficacy of adjuvant liposomes. (a) BALB/c mice bearing 4T1 tumors were treated with two weekly intratumoral injections of free or liposome-encapsulated MPL beginning on day 10 after intramammary injection of tumor cells (n = 5/group). Caliper-derived tumor measurements are presented (***p < 0.001 compared to vehicle control; $^{###}p$ < 0.001 compared to MPL liposomes; ^{++}p < 0.01 compared to IL-12). (b) IVIS imaging of tumor cell luciferase expression in mice following intraperitoneal injection with luciferin (75 mg/kg) before and after liposome treatment. (c) Photograph of excised tumors from three randomly selected mice from each group. (d) Mean weight of excised tumors on day 23. (e) Serum cytokine levels in control and liposome-treated mice 5 h postinjection, based on ELISA.

to cell-mediated immunity our goal was to boost the immune response further by adding rIL-12 to the liposome cocktail. IL-12, produced by macrophages and dendritic cells, stimulates proliferation and activation of cytotoxic $CD8^+$ lymphocytes and NK cells, leading to the production of IFN-γ, and stimulating antigen-specific and nonspecific immune responses.

Combined therapy with liposomal MPL and IL-12 (5 μg) was superior to either agent delivered independently with respect to inhibiting tumor growth. While control liposome treated tumors were similar in size to tumors in untreated animals, those treated with combination adjuvant were unchanged from the start of treatment based on caliper measurements (Figure 4a, n = 5/group) and were undetectable in some animals by bioluminescence (Figure 4b). An image of three randomly selected tumors from each group is presented in Figure 4c with the mean tumor weight and standard deviation of all animals in each group presented in Figure 4d. Serum cytokine measurements following single or combination therapy supported increases in IL-1β, IL-12, and TNF-α by all groups treated with adjuvant therapy, with a significant enhancement by combination over single agent therapy (Figure 4e). Only mice treated with IL-12 displayed an increase in serum IFN-γ.

Changes in the Cellular Phenotype of the Tumor Microenvironment. To study phenotypic changes and impact on cell growth in the tumor microenvironment following treatment with adjuvant particles, we analyzed tissue sections

dx.doi.org/10.1021/mp5002697 | Mol. Pharmaceutics 2014, 11, 3484−3491

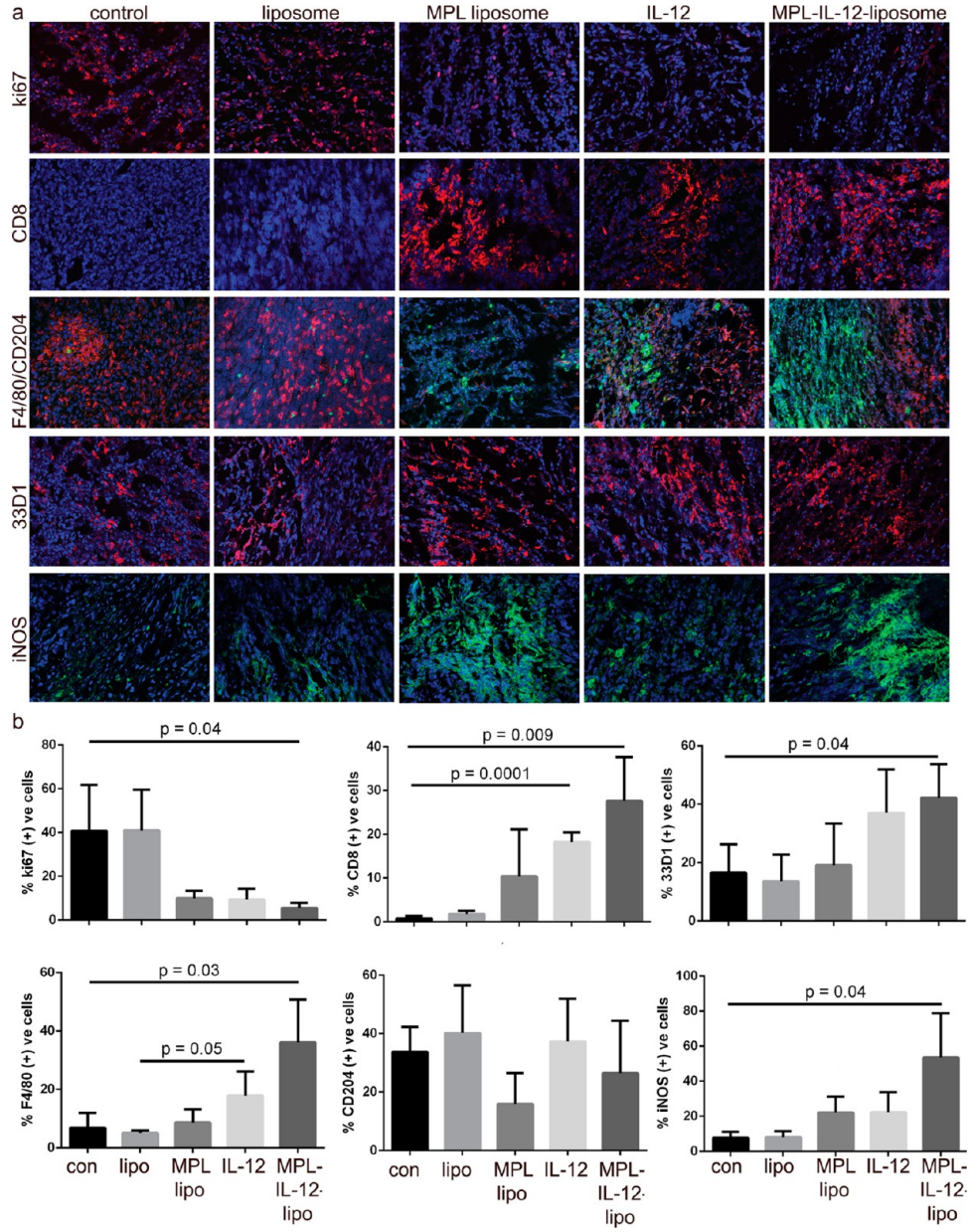

Figure 5. Cellular phenotype of tumors following adjuvant nanoparticle therapy. (a) Immunofluoresence staining of tumor sections from mice 2 weeks after initiation of liposome or IL-12 therapy [nuclei blue (DAPI), Ki67 red, CD8 red, F4/80 green, CD204 red, 33D1 red, and iNOS green]. (b) Percentage of immune cells in tumors based on manual, blinded cell counts in five randomly selected regions of interest (selected based on DAPI staining).

by immunofluorescence (Figure 5a,b). Cellular proliferation, based on K_i-67 expression, was similar for control and liposome treated animals (40%). However, the addition of MPL to the liposomes or injection with rIL-12 or MPL-IL-12-liposomes blocked proliferation (5−10%). The presence of CD8+ T cells in the tumor was negligible in control and liposome-treated mice (0.8%), as were F4/80 (7%) and iNOS (8%) expressing macrophages. Treatment with MPL-IL-12-liposomes led to significant increases in each of these populations (28%, 36%, and 54% for CD8+ T cells, F4/80, and iNOS macrophages), as well as in 33D1+ dendritic cells. The percentage of CD204 macrophages were not significantly altered in the tumors of mice treated with adjuvant liposomes. In conclusion, MPL-IL-12-liposomes augment infiltration of cytotoxic T cells and immune potentiating immune cells, and reduce proliferation of cells within the tumor.

Single Tumor Therapy in the Presence of Dual Tumors. MPL-IL-12-liposome therapy was administered to mice by intratumoral injection to induce cell death, block proliferation, and stimulate a cytokine and cellular milieu conducive to anticancer immunity. Since the presence of pro-inflammatory cytokines increased in the serum of treated mice, we sought to further document the presence of systemic anticancer immunity. Growth of distal, untreated tumors in mice receiving single tumor therapy was evaluated by caliper measurements of tumor volume (Figure 6a), tumor weight (Figure 6b), and bioluminescence (Figure 6c) based on luciferase expression in cancer cells. For all groups, growth of the distal tumor mirrored that of the treated tumor, with MPL-IL-12-liposome therapy having the greatest growth inhibitory effect.

dx.doi.org/10.1021/mp5002697 | *Mol. Pharmaceutics* 2014, 11, 3484−3491

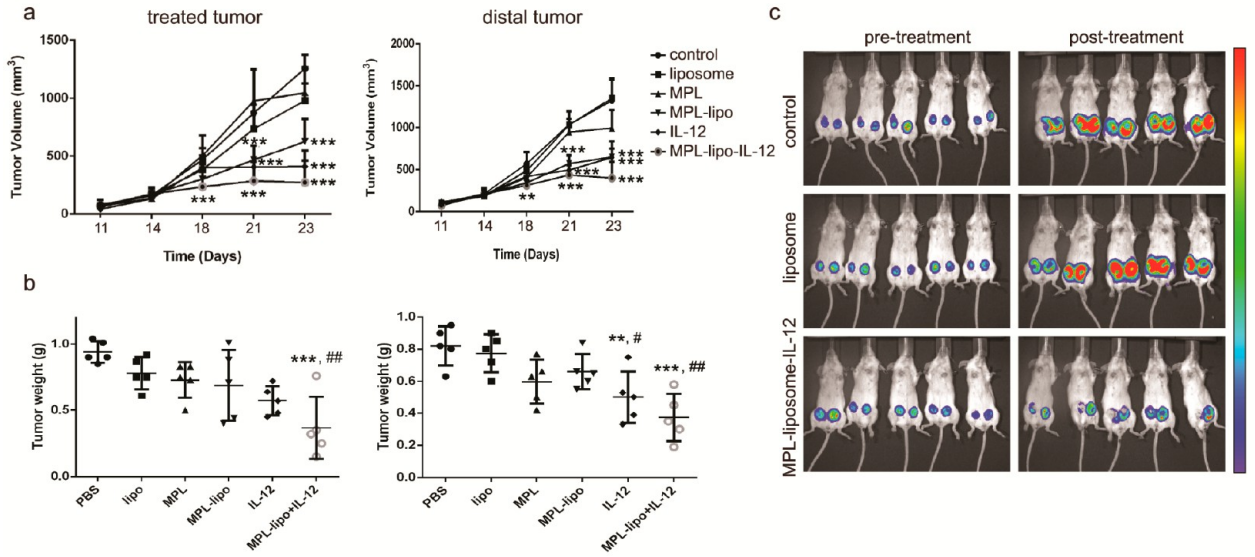

Figure 6. Impact of therapy on distal untreated tumor growth. BALB/c mice were injected with 4T1 cells in each inguinal fat pad (n = 5/group). When tumors were palpable, single tumors were treated by intramammary injection of liposomes, MPL, or IL-12 twice at weekly intervals. (a) Caliper measurements of treated and distal tumors (**p < 0.01, ***p < 0.001, compared to vehicle control). (b) Gross weights of excised tumors on day 23 (**p < 0.01, ***p < 0.001 compared to vehicle control; $^{\#}p$ < 0.05, $^{\#\#}p$ < 0.01 compared to liposome control). (c) IVIS imaging of tumor cell luciferase activity in select BALB/c groups on day 23.

DISCUSSION

While the addition of MPL to cationic liposomes did not alter the surface potential of the nanoparticles, the addition of IL-12 caused a 7 mV reduction in the zeta potential, supporting surface presentation of the cytokine. The advantage of nanoparticle-based presentation of IL-12 is reduction in serum levels, avoiding exposure to cytotoxic levels and permitting a more sustained, localized release.[18] The efficacy of using liposomal nanocarriers to reduce drug toxicity while enhancing immunity has also been demonstrated for other agents, such as amphotericin B in the fight against murine leishmaniasis.[19]

While both control and MPL liposomes were toxic to cancer cells as anticipated, injection of MPL liposomes, unlike control liposomes, reduced cellular proliferation in tumors. The decrease in proliferation may be attributed to increases in enzymes, such as iNOS, which was significantly upregulated in tumors following injection with MPL liposomes. Activation of APC with pathogens or pathogen-specific molecules (e.g., MPL) activates pathogen recognition receptors (PRRs), leading to release of effector molecules such as nitric oxide (NO) synthase (iNOS). NO has been shown to favor cell cycle arrest, mitochondria respiration, senescence, or apoptosis.[20] While resting immune cells lack expression of iNOS enzyme, TLR engagement with CD14-LPS (or MPL) complex activates intracellular signaling, which includes IRAK and MyD88 adaptors, leading to iNOS transcription.[21] Herein we demonstrate that MPL liposomes and IL-12 induce small increases in iNOS expression (3-fold), while combination therapy with IL-12 and MPL liposomes synergistically increase iNOS expression (7-fold).

In addition to releasing tumor antigen complexes, dying cancer cells release uric acid and lysosomal enzymes. These cellular components, as well as MPL, activate the Nod-like receptor protein 3 (NLRP3) inflammasome.[22,23] While NLRP3 activation has been linked to infiltration by DC and macrophages, we did not see significant increases in either 33D1^{+} DC or F4/80^{+} macrophages following treatment with MPL liposomes. However, when IL-12 was introduced into the liposomal formulation, there were large increases in DC, F4/80^{+} macrophages, and CD8^{+} T cells. NLRP3 activation stimulates secretion of IL-1β and IL-18.[24] We previously demonstrated that porous silicon particle-based presentation of MPL in mice bearing 4T1 tumors augments its ability to increase serum IL-1β levels, as well as other pro-inflammatory cytokines including IL-12, TNF-α, and IFN-γ.[16] In this study, MPL liposomes similarly increased serum levels of IL-1β, IL-12, and TNF-α. The addition of IL-12 lead to significantly greater increases in each of these cytokines and stimulated production of INF-γ.

Cytokine patterns elicited by activated T cells favor either cell-mediated immunity (i.e., T helper (Th)-1 biased), characterized by IFN-γ, IL-2 , and TNF-α, or humoral immunity (Th-2 biased), characterized by secretion of IL-4, IL-5, IL-6, and IL-10. IL-12 has potent antitumor effects and has been shown to direct immune reactions from Th-2 to Th-1.[25,26] As stated, IL-12 enhanced production of Th-1 cytokines and increased cytolytic T cells, DC, and F4/80^{+} macrophages, as well as iNOS. Intratumoral administration of combination IL-12 and MPL liposomes completely blocked 4T1 tumor growth. Combination liposomal therapy was able to induce similar reductions in tumor growth in both treated and distal tumors, suggesting a systemic immune response. Future studies will seek to differentiate specific antitumor immune responses from those resulting from general immune activation (e.g., cancer cell death due to TNF-α) and will seek to optimize particle-based accumulation of cytokines in the tumor, with an emphasis on studying dose effects and controlled, sustained presentation of cytokines for an optimal anticancer response with minimal cytotoxicity.

AUTHOR INFORMATION

Corresponding Author

*(R.E.S.) Phone: 713-798-3242. E-mail: ritaserda@gmail.com or rita.serda@bcm.edu.

Notes

The authors declare no competing financial interest.

■ ACKNOWLEDGMENTS

The authors thank Dr. Kenji Yokoi and Dr. Christian Celia for guidance with immunohistochemistry and liposome fabrication, respectively. We acknowledge and appreciate use of the Houston Methodist Research Institute Histology, Flow Cytometry, Microscopy, and Scanning Electron−Atomic Force Microscopy cores. The pseudo-colored lymphocyte image presented in the graphic abstract was acquired using a JEOL JSM-7800F field emission scanning electron microscope. This research was supported by the National Institutes of Health Grants U54 CA151668, U54CA143837, and NCATS TL1TR000369.

■ REFERENCES

(1) Lan, K. H.; Liu, Y. C.; Shih, Y. S.; Tsaid, C. L.; Yen, S. H.; Lan, K. L. A DNA vaccine against cytotoxic T-lymphocyte associated antigen-4 (CTLA-4) prevents tumor growth. *Biochem. Biophys. Res. Commun.* **2013**, *440* (2), 222−8.

(2) Wayteck, L.; Breckpot, K.; Demeester, J.; De Smedt, S. C.; Raemdonck, K. A personalized view on cancer immunotherapy. *Cancer Lett.* **2013**, *352*, 113−125.

(3) Jaime-Ramirez, A. C.; Mundy-Bosse, B. L.; Kondadasula, S.; Jones, N. B.; Roda, J. M.; Mani, A.; Parihar, R.; Karpa, V.; Papenfuss, T. L.; LaPerle, K. M.; Biller, E.; Lehman, A.; Chaudhury, A. R.; Jarjoura, D.; Burry, R. W.; Carson, W. E., 3rd. IL-12 enhances the antitumor actions of trastuzumab via NK cell IFN-gamma production. *J. Immunol.* **2011**, *186* (6), 3401−9.

(4) Phan, G. Q.; Rosenberg, S. A. Adoptive cell transfer for patients with metastatic melanoma: the potential and promise of cancer immunotherapy. *Cancer Control: Journal of the Moffitt Cancer Center* **2013**, *20* (4), 289−97.

(5) Wan, S.; Pestka, S.; Jubin, R. G.; Lyu, Y. L.; Tsai, Y. C.; Liu, L. F. Chemotherapeutics and radiation stimulate MHC class I expression through elevated interferon-beta signaling in breast cancer cells. *PloS One* **2012**, *7* (3), e32542.

(6) Audibert, F. Adjuvants for vaccines, a quest. *Int. Immunopharmacol.* **2003**, *3* (8), 1187−93.

(7) Craparo, E. F.; Bondi, M. L. Application of polymeric nanoparticles in immunotherapy. *Curr. Opin. Allergy Clin. Immunol.* **2012**, *12* (6), 658−64.

(8) Kool, M.; Soullie, T.; van Nimwegen, M.; Willart, M. A.; Muskens, F.; Jung, S.; Hoogsteden, H. C.; Hammad, H.; Lambrecht, B. N. Alum adjuvant boosts adaptive immunity by inducing uric acid and activating inflammatory dendritic cells. *J. Exp. Med.* **2008**, *205* (4), 869−82.

(9) Rimaniol, A. C.; Gras, G.; Clayette, P. In vitro interactions between macrophages and aluminum-containing adjuvants. *Vaccine* **2007**, *25* (37−38), 6784−92.

(10) Mori, A.; Oleszycka, E.; Sharp, F. A.; Coleman, M.; Ozasa, Y.; Singh, M.; O'Hagan, D. T.; Tajber, L.; Corrigan, O. I.; McNeela, E. A.; Lavelle, E. C. The vaccine adjuvant alum inhibits IL-12 by promoting PI3 kinase signaling while chitosan does not inhibit IL-12 and enhances Th1 and Th17 responses. *Eur. J. Immunol.* **2012**, *42* (10), 2709−19.

(11) Brewer, J. M. (How) do aluminium adjuvants work? *Immunol. Lett.* **2006**, *102* (1), 10−15.

(12) Braumuller, H.; Wieder, T.; Brenner, E.; Assmann, S.; Hahn, M.; Alkhaled, M.; Schilbach, K.; Essmann, F.; Kneilling, M.; Griessinger, C.; Ranta, F.; Ullrich, S.; Mocikat, R.; Braungart, K.; Mehra, T.; Fehrenbacher, B.; Berdel, J.; Niessner, H.; Meier, F.; van den Broek, M.; Haring, H. U.; Handgretinger, R.; Quintanilla-Martinez, L.; Fend, F.; Pesic, M.; Bauer, J.; Zender, L.; Schaller, M.; Schulze-Osthoff, K.; Rocken, M. T-helper-1-cell cytokines drive cancer into senescence. *Nature* **2013**, *494* (7437), 361−5.

(13) Meraz, I. M.; Hearnden, C. H.; Liu, X.; Yang, M.; Williams, L.; Savage, D. J.; Gu, J.; Rhudy, J. R.; Yokoi, K.; Lavelle, E. C.; Serda, R. E. Multivalent presentation of MPL by porous silicon microparticles favors T helper 1 polarization enhancing the anti-tumor efficacy of doxorubicin nanoliposomes. *PloS One* **2014**, *9* (4), e94703.

(14) Yan, W.; Chen, W.; Huang, L. Mechanism of adjuvant activity of cationic liposome: phosphorylation of a MAP kinase, ERK and induction of chemokines. *Mol. Immunol.* **2007**, *44* (15), 3672−81.

(15) Barnier-Quer, C.; Elsharkawy, A.; Romeijn, S.; Kros, A.; Jiskoot, W. Adjuvant effect of cationic liposomes for subunit influenza vaccine: influence of antigen loading method, cholesterol and immune modulators. *Pharmaceutics* **2013**, *5* (3), 392−410.

(16) Meraz, I. M.; Melendez, B.; Gu, J.; Wong, S. T.; Liu, X.; Andersson, H. A.; Serda, R. E. Activation of the inflammasome and enhanced migration of microparticle-stimulated dendritic cells to the draining lymph node. *Mol. Pharmaceutics* **2012**, *9*, 2049−2062.

(17) *FACSDIVA Software*, V6.0; BD Biosciences: San Jose, CA, 2007.

(18) Simpson-Abelson, M. R.; Purohit, V. S.; Pang, W. M.; Iyer, V.; Odunsi, K.; Demmy, T. L.; Yokota, S. J.; Loyall, J. L.; Kelleher, R. J., Jr.; Balu-Iyer, S.; Bankert, R. B. IL-12 delivered intratumorally by multilamellar liposomes reactivates memory T cells in human tumor microenvironments. *Clin. Immunol.* **2009**, *132* (1), 71−82.

(19) Daftarian, P. M.; Stone, G. W.; Kovalski, L.; Kumar, M.; Vosoughi, A.; Urbieta, M.; Blackwelder, P.; Dikici, E.; Serafini, P.; Duffort, S.; Boodoo, R.; Rodriguez-Cortes, A.; Lemmon, V.; Deo, S.; Alberola, J.; Perez, V. L.; Daunert, S.; Ager, A. L. A targeted and adjuvanted nanocarrier lowers the effective dose of liposomal amphotericin B and enhances adaptive immunity in murine cutaneous leishmaniasis. *J. Infect. Dis.* **2013**, *208* (11), 1914−22.

(20) Napoli, C.; Paolisso, G.; Casamassimi, A.; Al-Omran, M.; Barbieri, M.; Sommese, L.; Infante, T.; Ignarro, L. J. Effects of nitric oxide on cell proliferation: novel insights. *J. Am. Coll. Cardiol.* **2013**, *62* (2), 89−95.

(21) Lowenstein, C. J.; Padalko, E. iNOS (NOS2) at a glance. *J. Cell Sci.* **2004**, *117* (Pt 14), 2865−7.

(22) Martinon, F.; Petrilli, V.; Mayor, A.; Tardivel, A.; Tschopp, J. Gout-associated uric acid crystals activate the NALP3 inflammasome. *Nature* **2006**, *440* (7081), 237−41.

(23) Hornung, V.; Bauernfeind, F.; Halle, A.; Samstad, E. O.; Kono, H.; Rock, K. L.; Fitzgerald, K. A.; Latz, E. Silica crystals and aluminum salts activate the NALP3 inflammasome through phagosomal destabilization. *Nat. Immunol.* **2008**, *9* (8), 847−56.

(24) Dinarello, C. A. Interleukin 1 and interleukin 18 as mediators of inflammation and the aging process. *Am. J. Clin. Nutr.* **2006**, *83* (2), 447S−455S.

(25) Manetti, R.; Parronchi, P.; Giudizi, M. G.; Piccinni, M. P.; Maggi, E.; Trinchieri, G.; Romagnani, S. Natural killer cell stimulatory factor (interleukin 12 [IL-12]) induces T helper type 1 (Th1)-specific immune responses and inhibits the development of IL-4-producing Th cells. *J. Exp. Med.* **1993**, *177* (4), 1199−204.

(26) Sypek, J. P.; Chung, C. L.; Mayor, S. E.; Subramanyam, J. M.; Goldman, S. J.; Sieburth, D. S.; Wolf, S. F.; Schaub, R. G. Resolution of cutaneous leishmaniasis: interleukin 12 initiates a protective T helper type 1 immune response. *J. Exp. Med.* **1993**, *177* (6), 1797−802.